TIE-LINE BASED PARAMETERIZATION FOR THERMAL COMPOSITIONAL RESERVOIR SIMULATION

A REPORT
SUBMITTED TO THE DEPARTMENT OF ENERGY RESOURCES ENGINEERING
OF STANFORD UNIVERSITY
IN PARTIAL FULFILLMENT OF THE REQUIREMENTS
FOR THE DEGREE OF
MASTER OF SCIENCE

By

Alireza Iranshahr

June 2008

© Copyright by Alireza Iranshahr 2008

All Rights Reserved

I certify that I have read this report and that in my opinion it is fully adequate, in scope and in quality, as partial fulfillment of the degree of Master of Science in Petroleum Engineering.

Hamdi Tchelepi Principal Advisor

Abstract

Thermodynamic equilibrium computations are usually the most time consuming component in compositional reservoir flow simulation. A Compositional Space Adaptive Tabulation (CSAT) approach has been developed in order to speed up the Equation of State (EoS) computations. The methodology adaptively parameterizes the compositional space using a small number of tie-lines, which are assembled into a table. The phase equilibrium information for a composition is interpolated from the tie-line table. In this work, we extend the CSAT approach to thermal problems. Given an overall composition at a fixed temperature, the boundary between sub- and super-critical pressures is represented by the critical tie-line and the corresponding minimal critical pressure. A small set of sub-critical tie-lines is computed and stored for a given temperature. This process is repeated for the pressure and temperature ranges of interest, and a regular tie-line table is constructed. Close to the critical boundary, a refined tie-line table is used for phase identification. A combination of regular and refined interpolation improves the robustness of the tie-line search procedure and the overall efficiency of the computations. Several challenging tests are used to demonstrate the robustness and efficiency of this general thermal-compositional tie-line based parameterization method. Our results indicate that CSAT provides very accurate treatment of the near-critical region with a small number of preconditioned EoS flash iterations. Moreover, the computational efficiency of the method is at least an order of magnitude better than that of standard EoS-based approaches. We also show that the efficiency gains relative to standard techniques increase with the number of gridblocks in the simulation model.

Acknowledgement

I take this opportunity to thank my research and academic advisor, Prof. Hamdi Tchelepi, for his insightful ideas and invaluable input to this work. Without his intelligent feedback, this work would not have been finished. I particularly appreciate the freedom he offered me, so that I got one more step closer to becoming an innovative researcher. I am really privileged that I will continue to explore a more challenging academic period under his guidance.

I am also grateful to Dr. Denis Voskov for his valuable advice and critical ideas. He introduced me to the compositional module of GPRS (Stanford's General-Purpose Research Simulator), which is the most comprehensive simulator I have ever worked with, and he helped me design the most efficient implementation I have achieved so far.

I also thank Chevron Energy Technology Company for providing me the opportunity to perform numerous real field simulations, which revealed the shortcomings of the initial implementation. Financial support from the Stanford University Petroleum Research Institute program for Reservoir Simulation (SUPRI–B) is greatly acknowledged.

Finally, as a trivial effort to honor their everlasting love and support, I dedicate this work to my beloved parents, Manouchehr and Manijeh Iranshahr.

Alireza Iranshahr

June, 2008

Contents

Abstract **iv**

Acknowledgement **v**

List of Tables **viii**

List of Figures **ix**

1 Introduction **1**

1.1 Standard EoS calculations 2

1.2 Analytical Theory of Gas Injection Processes 4

1.2.1 Formulation 4

1.2.2 Solution Route Construction 8

1.2.3 Multi-contact miscible displacements 9

2 Compositional Space Adaptive Tabulation **11**

2.1 Introduction 11

2.2 Tie-Line Based Parameterization 12

2.2.1 Phase Behavior Representation Using Compositional Space Parameterization 14

2.3 Compositional Parameterization for Isothermal Problem 17

2.3.1 Parameterization of Sub-critical Problems 18

2.3.2 Parameterization of the Super-critical Region 21
2.3.3 Combining Super-critical State Criteria with Sub-critical State Parameterization 24
2.4 Tie-Line Parameterization of Thermal Problems 24
2.4.1 Parameterization of Sub-critical Thermal Problems 25
2.4.2 Parameterization of Super-critical Thermal Problem 29
2.4.3 Parameterization for General-purpose Thermal Compositional Simulation 29

3 Implementation and Numerical Results **31**
3.1 Implementation 31
3.1.1 Tie-line Table Construction 31
3.1.2 Critical Tie-line Table Check 34
3.1.3 Sub-critical Tie-line Check 35
3.2 Numerical Examples 36
3.2.1 Thermal CSAT Accuracy, Case Study 38
3.2.2 Thermal CSAT, Application to Compositional Flow Simulation . . . 42

4 Conclusions **47**

Bibliography **48**

A User's Guide to CSAT in GPRS **53**
A.1 Keywords 53
A.2 Simulation Output 55

List of Tables

3.1 CSAT efficiency for depletion below the bubble point, CPU time is reported in (hr:min) 37

3.2 Isothermal CSAT vs. standard approach: sensitivity to number of components, CPU time is reported in seconds 38

3.3 Composition and properties of the test mixture [21] 39

3.4 Tie-line table parameters 39

3.5 Calls (x10^5) to various interpolation routines of thermal CSAT for SPE3 (top) and SPE5 (bottom); values in parentheses indicate the percentage of positive identification based on (2.13) from the total calls to the routine. Since the critical check is performed in the first level, summation of all positive identifications equals the total calls to the critical check tests. 45

3.6 Ratio (standard/CSAT) of SSI and Newton stability tests for SPE3 and SPE5 46

List of Figures

1.1 Non tie-line paths for concave envelope curve on liquid side (top) and vapor side (bottom) (modified from [7, page 253]) 9

1.2 Non tie-line paths for convex envelope curve on liquid side (top) and vapor side (bottom) (modified from [7, page 254]) 9

2.1 Binodal surface at different $p-T$ conditions for $\{C_1, CO_2, C_4, C_{10}\}$ 16

2.2 Binodal surface at an intermediate $p-T$ condition 16

2.3 Calculation of tie-lines through a base point at different pressure levels with $N_p = 4$ (left); associated tie-line table (right) 18

2.4 Table look-up and adaptive construction strategy for sub-critical compositions 20

2.5 Tie-lines in coarse table (blue squares) and in refined table (red circles) for an isothermal tie-line table 21

2.6 Space parameterization using critical tie-lines 22

2.7 Adaptive Super-critical State Criteria (SSC) 23

2.8 Generic tie-line table structure on $p-T$ grid, none of the temperature values (left), some of them (center) or all of them (right) contain an MCP. Note the construction of the additional refined table in the second case. Pressure and temperature bounds are defined by the black frame. 27

2.9 Refined interpolation, four tie-lines at the corners of the parallelogram are used for interpolation 28

2.10 Sub-critical interpolation framework, test point could be anywhere along the horizontal dashed line 30

3.1 Variation of tie-line length in the near-critical region, the binary search returns a result bounded by the curly bracket 32
3.2 Fracture network of the model used for case studies 36
3.3 Negative flash with initial guess from space tabulation and standard procedures 40
3.4 Negative flash with initial guess from space tabulation (red) and phase stability test (blue): sensitivity to temperature; Tables of tie-lines are computed at different temperatures 41
3.5 Space tabulation: sensitivity to coarseness in temperature tabulation 42
3.6 Base case I: temperature and composition profiles (left), solution path in compositional space(right) with binodal surfaces at initial and injection conditions 43
3.7 Base case II: temperature and composition profiles (left), solution path (right) 44
3.8 Thermal CSAT performance for SPE3 (left) and SPE5 (right), EoS time for CSAT based simulations is a weak function of grid size 46

Chapter 1

Introduction

Enhanced oil recovery (EOR) methods are used to increase the amount of oil extracted from reservoirs after primary and secondary recovery operations. Miscible and near-miscible gas injection processes and steam flooding are among the most commonly used EOR methods. In gas injection processes, for example, mass transfer between the lighter injected gas and the heavier resident oil improves the local displacement efficiency. Important production decisions are made based on the insights obtained from simulation studies of these complex displacement processes. As a result, accurate modeling of EOR processes, which are often compositional, is essential for planning field projects and managing production operations.

The standard approach for solving the equations that describe the conservation of mass and energy and the phase equilibrium relations is based on solving the coupled problem in two stages. In one of these stages, the phase equilibrium computations are usually performed separately using an Equation of State (EoS). The EoS calculations usually include (1) a stability test to determine the phase state and (2) flash computations to determine phase amounts and compositions, when multiple phases are present. The computational cost of compositional simulation grows with the number of components used to represent the fluid system and the number of gridblocks in the reservoir model. As a result, while

computer capabilities have grown substantially, high-resolution compositional simulation of field-scale displacements is far from being routine practice.

Recently, several research efforts have been made to overcome the computational complexities of standard approaches [7]–[16]. In this report, we focus on methods that employ tie-line based parameterization of the compositional space. The first version of a general-purpose tie-line based compositional research simulator suggests significant efficiency in modeling two-phase isothermal problems with large numbers of components [14]–[16]. In this work, we extend the Compositional Space Adaptive Tabulation (CSAT) appraoch in two ways: by showing that it is, in fact, applicable to large-scale compositional displacement problems, and by extending CSAT to thermal-compositional reservoir simulation.

In this chapter, we briefly review previous work on modeling compositional displacement processes in porous media. Standard and analytical tie-line based approaches are considered to build up a conception of our general-purpose compositional space tabulation methodology. The tie-line based approach is discussed in more detail, since it provides better insight into the mechanisms of compositional displacements and is the basis for many of the fundamental advances presented in this thesis. The details of the isothermal tabulation techniques and extension to thermal problems are presented in Chapter 2. In Chapter 3, we summarize the algorithms of space parameterization in terms of pseudo-code, and we explain the accuracy and efficiency of CSAT using a variety of numerical examples.

1.1 Standard EoS calculations

The equations governing compositional displacements in porous media are the mass conservation equations, one per component, and phase equilibrium relations, which describe how components partition across the various fluid phases. The reservoir is discretized into

computational gridblocks (control-volumes), and the governing equations are discretized accordingly. The resulting nonlinear equations are coupled. The mass balance equations (primary equations) describe the interactions between different gridblocks, and phase equilibrium equations depend only on the variables in a given gridblock.

A two-stage strategy is used to solve the overall problem. Namely, the flow equations, which are coupled over the entire spatial domain, are solved. At this stage, thermodynamic effects are held 'fixed'. Once the flow part of the system has been updated, the thermodynamic state (phase fractions and compositions) of each gridblock is determined separately. These two stages are performed within a Newton iteration for a timestep in the simulation. The procedures are repeated until the entire set of flow and thermodynamic equations converge to a solution for the timestep.

Two types of standard Equation of State (EoS) based calculations are involved during the simulation of compositional problems: phase–state stability test and standard flash computations. A detailed discussion of both procedures is provided in reference [4, chapter 4]. These computations are required for each gridblock during every Newton iteration of a timestep. This is because changes in the solution variables and alignment of primary and secondary equations may be required, when the number of phases present in a gridblock changes during the simulation.

The phase stability test is performed for all single-phase cells to determine if the state of the composition is stable under the prevailing pressure and temperature conditions. If it is found to be unstable, standard flash calculations are performed to determine the phases and their compositions. The results of the stability test can be used as an initial guess for flash computations [5]. In most simulators, the phase stability test can become the dominant kernel in EoS computations.

1.2 Analytical Theory of Gas Injection Processes

A method of characteristics (MoC) based approach for two–phase multi–component displacements has been derived for ideal problems [7]. In this section, we briefly present how analytical solutions of gas injection problems can be constructed. This approach is valid under ideal conditions; it is assumed that the displacement takes place at constant pressure and temperature in a one-dimensional homogeneous porous medium without any dispersion.

We first define the basic terminology associated with this theory. For n_c components at a fixed temperature and pressure, the space of all composition points can be represented using an $(n_c - 1)$ dimensional space,

$$\mathcal{S}^{n_c} = \{(z_i)_{1\leq i\leq n_c} \in [0,1]^{n_c} \Big| \sum_i z_i = 1\}. \tag{1.1}$$

The bubble and dew surfaces are constructed from equilibrium points at liquid and vapor states, respectively. These binodal curves envelop the two-phase region. A *tie-line* connects two points, one on the dew-point surface and one on the bubble-point surface. The two surfaces meet at the *critical locus*, where the length of the tie-lines is zero. No tie-lines exist above the critical region, by definition. Thus, the entire compositional space is divided into a *sub-critical* region, where tie-lines and their extensions are defined, and a *super-critical* region.

1.2.1 Formulation

We begin by formulating the eigenvalue problem for a multi-component displacement. Assuming incompressible flow, we have $n_c - 1$ independent conservation equations:

$$\frac{\partial C_i}{\partial \tau} + \frac{\partial F_i}{\partial \xi} = 0, \qquad i \in \{1, n_c - 1\}, \tag{1.2}$$

where C_i is the overall concentration and F_i is the overall fractional flow of component i. These quantities are defined as

$$\begin{aligned} C_i &= x_i L + y_i(1-L), \\ F_i &= x_i f + y_i(1-f), \end{aligned} \tag{1.3}$$

where x and y are the compositions of the bubble and dew points, respectively; L and f represent, respectively, the mole fraction and fractional-flow of the liquid phase. Writing F_i as a function of the $n_c - 1$ independent compositions, we have

$$\frac{\partial F_i}{\partial \xi} = \sum_{j=1}^{n_c-1} \frac{\partial F_i}{\partial C_j} \frac{\partial C_j}{\partial \xi}. \tag{1.4}$$

Substitution of (1.4) into (1.2) and defining $\mathbf{u} = [C_1, C_2, \ldots, C_{n_c-1}]^T$, we get:

$$\frac{\partial \mathbf{u}}{\partial \tau} + A(\mathbf{u}) \frac{\partial \mathbf{u}}{\partial \xi} = 0, \tag{1.5}$$

where:

$$A(\mathbf{u}) = \begin{pmatrix} \frac{\partial F_1}{\partial C_1} & \frac{\partial F_1}{\partial C_2} & \cdots & \frac{\partial F_1}{\partial C_{n_c-1}} \\ \frac{\partial F_2}{\partial C_1} & \frac{\partial F_2}{\partial C_2} & \cdots & \frac{\partial F_2}{\partial C_{n_c-1}} \\ & & \ddots & \\ \frac{\partial F_{n_c-1}}{\partial C_1} & \frac{\partial F_{n_c-1}}{\partial C_2} & \cdots & \frac{\partial F_{n_c-1}}{\partial C_{n_c-1}} \end{pmatrix}. \tag{1.6}$$

We are interested in finding the trajectory of a certain composition in space and time. Therefore,

$$dC_i = \frac{\partial C_i}{\partial \tau} d\tau + \frac{\partial C_i}{\partial \xi} d\xi = 0, \tag{1.7}$$

must be satisfied for each component along the trajectory. Rearranging (1.7) yields:

$$\frac{\partial \mathbf{u}}{\partial \tau} = -\lambda \frac{\partial \mathbf{u}}{\partial \xi}, \tag{1.8}$$

where $\lambda = \frac{d\xi}{d\tau}$. Combining (1.8) with (1.5) results in:

$$(A(\mathbf{u}) - \lambda I) \frac{\partial \mathbf{u}}{\partial \xi} = 0. \tag{1.9}$$

Equation (1.9) is satisfied only if $\det[A(\mathbf{u}) - \lambda I] = 0$, where λ represents the eigenvalues of $A(\mathbf{u})$. Thus, each composition point in the two-phase region has $n_c - 1$ eigenvalues. Physically, the pair of eigenvectors and eigenvalues at a composition point define, respectively, possible directions and associated velocities of the composition wave in the space. It can be shown that the tie-line through the composition point is itself a legitimate composition path [7, page 181]. The other $n_c - 2$ eigenpairs represent *non tie-line* paths through the composition point. Explicit relations for non tie-line paths have been derived for three- and four-component mixtures, when equilibrium K-values are constant [7, pages 115 and 187].

Tie-line and non tie-line paths for a three-component system with constant K-values are given in [7, figure 5.8, page 119], for example. Along each tie-line path, there are two points where the eigenvalue of the tie-line path is equal to that of the non tie-line path. Non tie-line paths are tangent to the tie-line at these *equal-eigenvalue points*, and any switch from a tie-line path to a non tie-line path must take place at these points. It can be shown that there are $2(n_c - 2)$ equal-eigenvalue points along each tie-line in a system of n_c components.

Shocks and Rarefactions

The solution path between initial and injection composition points involves a set of *key tie-lines*, *shocks* and *rarefactions* of non tie-line path between key tie-lines. When the change in the compositions is continuous along a portion of the composition path (rarefaction), the velocities of composition waves must increase monotonically from upstream to downstream. This is called the *velocity constraint* and ensures a single-valued solution where ever it is satisfied. However, there are situations where continuous variation along non tie-line rarefaction leads to unphysical results, since eigenvalues along a non tie-line path decrease as the path is traced from upstream towards downstream. In such cases, discontinuities (shocks) in concentration are introduced to maintain a physical single-valued solution. A shock must satisfy the *entropy condition*, which compares the shock velocity

(Λ) with immediate upstream and downstream wave velocities:

$$\lambda^{downstream} \leq \Lambda \leq \lambda^{upstream}. \tag{1.10}$$

There are two kinds of shocks: (1) Shocks that connect a single-phase composition with a two-phase composition. These shocks arise when the solution path enters or leaves the two-phase region, and they occur along the extension of a tie-line [7, page 124]. (2) Shocks which connect two points in the two-phase region. It can be shown that these points lie on two 'key' tie-lines, and that the extension of these two tie-lines must intersect [7, page 131]. Since the calculation of key tie-lines plays an important role in the construction of the solution route, we first consider how the key tie-lines are determined for a multi-component system.

Key Tie-lines

When the equilibrium K-values are independent of composition, the solution path in compositional space satisfies several special properties. It can be shown that a planar surface can be constructed from the set of all intersecting tie-lines in the compositional space. Each composition is associated with $n_c - 2$ non tie-line paths, and a particular tie-line is intersected by a set of $n_c - 2$ non tie-line paths. Each one of these sets lie on a separate plane of tie-lines. Moreover, the shock that connects two tie-lines in the two-phase region lies in the plane where the two tie-lines reside [6]. Therefore, the composition path between injection and initial composition points traverses planes of tie-lines, and the key tie-lines can be computed by intersecting planes of tie-lines.

However, when the K-values are not constant, the surface of tie-lines, which also contains a set of non tie-line paths is a *ruled surface* rather than a plane. In this case, the non tie-line paths are obtained by piecewise integration along the non tie-line direction [7, page 200].

Key tie-lines are computed via simultaneous solution of tie-line intersection equations:

$$x_i^n\{L^n(1-K_i^n)+K_i^n\} = x_i^{n+1}\{L^{n+1}(1-K_i^{n+1})+K_i^{n+1}\}, \tag{1.11}$$

In these equations, subscript $i \in \{1, n_c-1\}$ refers to the components and superscript $n \in \{1, n_c-2\}$ refers to the key tie-lines. It should be noted that the liquid phase fraction at the intersection point is different for each of the intersecting tie-lines. For example, each of the initial and injection 'key' tie-lines must satisfy

$$z_i = x_i\{L(1-K_i)+K_i\}, \qquad i \in \{1, n_c-1\}, \tag{1.12}$$

where **z** indicates the compositions of initial or injection points. Different approaches have been proposed for the solution of this highly nonlinear system of equations (1.11) [1, 2, 3].

1.2.2 Solution Route Construction

Once the key tie-lines for a compositional system have been computed, one should determine if the path between any two adjacent key tie-lines is a rarefaction, or a shock. This question has been carefully studied for various configurations of key tie-lines [7, page 249]. Figures (1.1) and (1.2) summarize all possible arrangements. It can be shown that the construction of the solution route is most straightforward, if it begins from the shortest key tie-line [7, page 246]. Specific algorithmic steps for the treatment of fully self-sharpening displacements and displacements with non tie-line rarefaction are given in reference [7, pages 256 and 260].

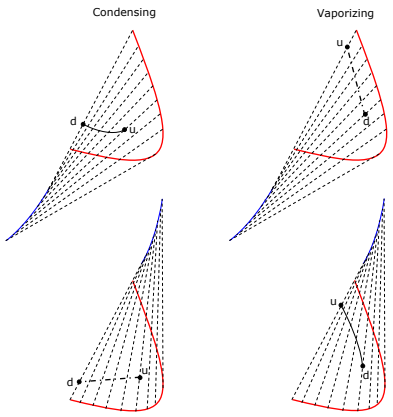

Figure 1.1: Non tie-line paths for concave envelope curve on liquid side (top) and vapor side (bottom) (modified from [7, page 253])

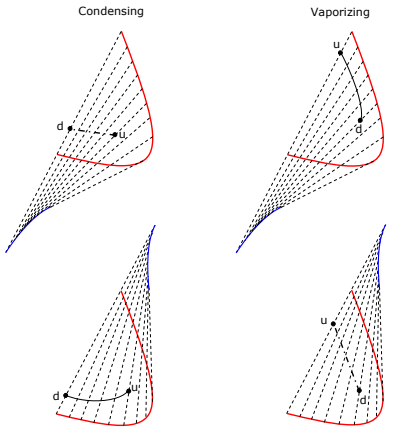

Figure 1.2: Non tie-line paths for convex envelope curve on liquid side (top) and vapor side (bottom) (modified from [7, page 254])

1.2.3 Multi-contact miscible displacements

The efficiency of a gas injection process depends on the structure of the two-phase binodal surface and the relative configuration of the key tie-lines. Traversal of the solution route inside the two-phase region reduces the displacement efficiency by leaving some oil behind.

Consider the immiscible displacement shown in [7, figure 5.22, page 155]. Shock velocities for this fully self-sharpening system indicate that enriching the initial oil with intermediate components slows the leading shock and speeds up the trailing shock. Also, the saturation profiles show that the amount of oil present in the two-phase region decreases. In the limit when the initial tie-line is the critical one, all three shocks unite in a single shock, which moves with unit velocity and results in piston-like displacement of oil.

A similar effect could be achieved if the displacement pressure is increased so that the binodal surface shrinks, and the initial tie-line becomes the critical one. The displacement becomes miscible after the pressure reaches the minimum miscibility pressure (*MMP*). The solution route for such a displacement never enters the two-phase region. Extending the same ideas to systems of many components, one concludes that a displacement is multi-contact miscible, if any of the $(n_c - 1)$ key tie-lines is a critical tie-line. Based on this fact, an iterative search procedure can be designed to calculate the *MMP*. Starting from a low pressure, key tie-lines are computed by solving (1.11). If all key tie-line have non-zero length, the pressure is incremented until one of the key tie-lines converge to a point. The corresponding pressure is the *MMP*.

In fact, many practical compositional problems involve solution routes along critical tie-lines, which can lead to modeling challenges as we will see later.

Chapter 2

Compositional Space Adaptive Tabulation

In this chapter, we introduce tie-line based parameterization of the compositional space for multi-component multiphase thermal displacement processes. After a brief description of the methodology for isothermal compositional simulation, we focus on the generalization to thermal problems.

2.1 Introduction

As discussed in the previous chapter, analytical solutions based on the Method of Characteristics can be derived for two-phase multi-component gas injection problems. The theoretical approach is applicable to homogeneous one-dimensional dispersion-free problems under constant p and T conditions [7]. Obviously, these restrictions are quite significant for a general thermal compositional problem. In this chapter, we briefly describe how a tie-line based parameterization approach can be used to obtain a general-purpose simulation framework for thermal compositional displacements in multi-dimensional heterogeneous reservoirs.

There are several related research efforts similar to the parameterization procedure described here. Wang et al. [18] formulated a compositional reservoir simulator using an IMplicit Pressure, Explicit Compositions (IMPEC) approach. They employ negative flash [7, page 48] to perform both phase–state identification and flash calculations. For their method to be efficient, however, a good initial guess for the negative flash is required. Rasmussen et al. [19] proposed a method to perform the phase stability test and flash calculations more efficiently for compositional mixtures in pipe flow. Their criteria avoid the stability test for single phase fluids. Pope [20] proposed the In Situ Adaptive Tabulation method for efficient modeling of turbulent reactive combustion, in which the compositional space is tabulated and adaptively updated. However, the nature of that problem is completely different from ours.

2.2 Tie-Line Based Parameterization

Efficient parameterization of the compositional space is a challenging problem. Based on the results of the MoC-based solution to ideal compositional problems, it is clear that tie-lines are suitable candidates for parameterization [7]. The theory for gas injection processes presented in [7] has largely improved our knowledge of the thermodynamic and hydrodynamic interactions in compositional porous media flows. Motivated by this theory, a tie-line based parameterization method has been developed, which treats the thermodynamic portion of the problem using tie-lines rather than the conventional representation of the compositional space [8]–[13]. In this section, we briefly present this approach.

The overall composition, $\mathbf{z}$, of all points along a particular tie-line can be expressed in terms of the equilibrium compositions $(\mathbf{x}, \mathbf{y})$, which define the end-points of a tie-line in the n_c-compositional space:

$$z_i = x_i L + y_i(1 - L), \qquad i \in \{1, n_c\}. \tag{2.1}$$

Using this equation, individual overall compositions can be written in terms of the composition of a *primary component*, k, as: [8]

$$z_i = A_i z_k + B_i, \qquad i \in \{1, n_c\}\backslash\{k\}, \tag{2.2}$$

where:

$$A_i = \frac{x_i - y_i}{x_k - y_k} \qquad \text{and} \qquad B_i = y_i - y_k A_i. \tag{2.3}$$

The $n_c - 1$ parameters (A_i, B_i) uniquely define the tie-line through a composition point at constant p and T. Based on this fact, one can replace the composition vector, $\mathbf{z} = (z_i)_{i\in\{1,n_c\}}$ of a point with a new set of independent variables (z_k, Γ), where the $(n_c - 1)$–dimensional vector $\Gamma = (\gamma_i)_{i\in\{1,n_c\}\backslash\{k\}}$ uniquely represents a particular tie-line. As a result, any arbitrary parameter can be used to represent Γ as long as it is unique for each tie-line. A convenient choice is the center point of the tie-line [13]. The equilibrium phase compositions associated with each tie-line are then tabulated in terms of the chosen parameter. A set of tie-lines represented by Γ (which define Γ**-space**) can be chosen to provide a discrete representation of the tie-line space.

The new variable set facilitates parameterization of the compositional space in terms of tie-lines. This parameterization allows the splitting of the compositional displacement problem into thermodynamic and hydrodynamic parts [8]. Consider the system of conservation equations for incompressible two-phase flow of a compositional fluid in a 1D porous medium:

$$\frac{\partial z_i}{\partial \tau} + \frac{\partial F_i}{\partial \xi} = 0, \qquad i \in \{1, n_c - 1\}, \tag{2.4}$$

where the overall fractional flow of component i, F_i, can be expressed in terms of tie-line parameters A_i and B_i:

$$F_i = A_i F_k + B_i, \qquad i \in \{1, n_c - 1\}\backslash\{k\}. \tag{2.5}$$

Using parameterization in terms of z_k and γ_i, (2.4) can be decoupled as follows:

$$\begin{aligned} \frac{\partial z_k}{\partial \tau} + \frac{\partial F_k}{\partial \xi} &= 0, \\ \frac{\partial (A_i z_k + B_i)}{\partial \tau} + \frac{\partial (A_i F_k + B_i)}{\partial \xi} &= 0, \qquad i \in \{1, n_c - 1\} \backslash \{k\}. \end{aligned} \tag{2.6}$$

This Riemann problem can be solved by splitting it into two successive Riemann subproblems, namely, thermodynamic and hydrodynamic parts [8, 9]. The thermodynamic problem is cast in terms of tie-line parameters, A_i and B_i:

$$\frac{\partial A_i(\gamma)}{\partial \tau} + \frac{\partial B_i(\gamma)}{\partial \zeta} = 0, \qquad i \in \{1, n_c - 1\} \backslash \{k\}. \tag{2.7}$$

The solution to this problem is only a function of the thermodynamic behavior of the system. It can be shown that the solution path in Γ-space is independent of the variations in hydrodynamic variables. This fact has also been proved for compressible flow [10, 12].

Reformulating (2.6) in terms of the concentration and any parameter along the solution path in Γ-space (which is obtained from (2.7)) leads to the following hydrodynamic problem:

$$\begin{aligned} \frac{\partial z_k}{\partial \tau} + \frac{\partial F_k}{\partial \xi} &= 0, \\ \frac{\partial (A_j(\gamma) z_k + B_j(\gamma))}{\partial \tau} + \frac{\partial (A_j(\gamma) F_k + B_j(\gamma))}{\partial \xi} &= 0. \end{aligned} \tag{2.8}$$

This system can be solved using conventional methods for the solution of oil displacement problems [8]. The methodology has been implemented for multidimensional problems, where the Γ-space has been parameterized using polynomial interpolation [10, 12].

2.2.1 Phase Behavior Representation Using Compositional Space Parameterization

Projecting the phase equilibrium compositions onto the standard compositional space generates the binodal surface for the system at fixed $p - T$ conditions. Here, we consider a

tie-line based representation of the phase behavior. For the pressure (and temperature) interval of interest, the phase diagram is constructed using a fixed density of tie-lines [10, 12]. The tie-lines of the two-phase envelope can be computed using an appropriate EoS module [12, 13]. Delaunay triangulation is then used to construct a mesh for the compositional space [14].

Figure (2.1) shows the resulting binodal surface at different $p - T$ conditions for a four–component system. The two-phase envelope changes slowly as the pressure and temperature change gradually. Comparison of the binodal surface at an intermediate $p - T$ condition (figure 2.2) with those of figure (2.1) suggests that a good approximation to the intermediate surface can be generated from four surfaces by interpolating in both p and T. This interpolation can be performed for all intermediate $p - T$ conditions.

By discretizing the tie-line space using Delaunay triangulation, one can use natural neighbor interpolation [14] to compute the tie-line through a given composition point in the space of tie-lines. Linear interpolation in pressure (and temperature) can then be employed to obtain the tie-line at an intermediate condition. This test has been performed for $\{N_2, C_1, C_3, C_9\}$ at $p = 2300, 3000\, psia$ and $T = 270°\text{F}$. Repeating the procedure for a wide range of multi-component systems using random composition points, the largest error from this compositional space tabulation based flash was reported to be less than 1% [15].

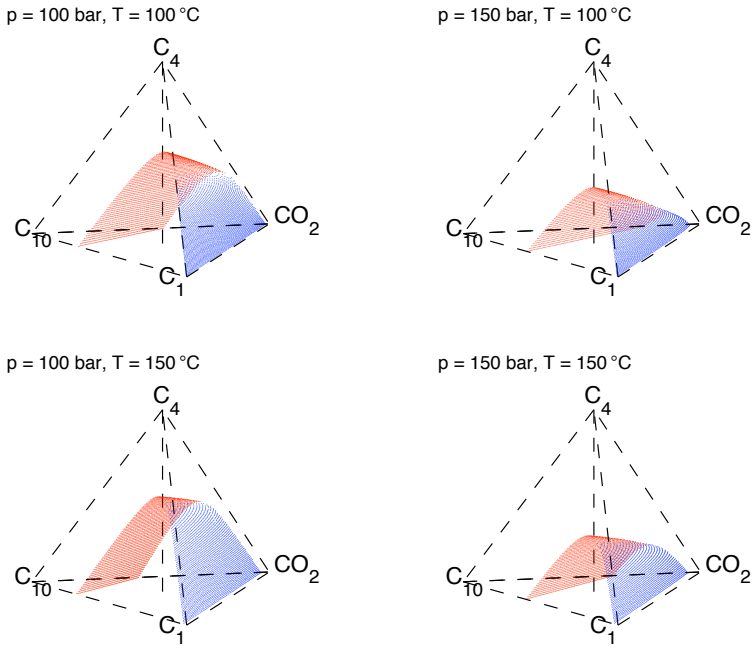

Figure 2.1: Binodal surface at different $p-T$ conditions for $\{C_1, CO_2, C_4, C_{10}\}$

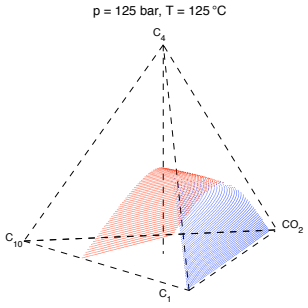

Figure 2.2: Binodal surface at an intermediate $p-T$ condition

However, computing and storing the entire binodal surface is an expensive and unnecessary task. This is because a multi-component gas injection displacement usually takes place in a small part of the compositional space [16]. As discussed before, for analytical problems the solution route in compositional space is along *tie-line* and *non tie-line* paths. Composition points in the two-phase region can be connected to single-phase points via a

tie-line path; while a non tie-line path defines the composition route inside the two-phase region. Since standard formulations of general-purpose compositional simulators perform a phase stability test (followed by standard flash, if applicable) for single-phase compositions, the main focus of our space parameterization is on tie-line paths. In gas injection problems, for example, injection and initial compositions are often in the single phase region and the solution path connecting them involves the injection and initial tie-lines.

For general compositional problems, pressure changes along the solution path. In the presence of numerical dispersion, the single-phase composition points may deviate from the injection and initial tie-lines, and the idea of composition paths along key tie-lines may not be applicable. However, as shown before, since the phase behavior of the system defined by the two-phase binodal surface is a weak function of pressure (at least for pressures below the critical locus) the composition path in single-phase regions is close to key tie-lines *within a tolerance*. Numerical experiments indicate that the number of additional computed tie-lines between the injection and initial tie-lines is small [13, 14]. This suggests generalization of similar ideas to practical compositional problems. In fact, even for very complicated compositional problems, the solution route in compositional space involves a limited number of tie-lines.

2.3 Compositional Parameterization for Isothermal Problem

In this section, we briefly review the compositional space parameterization framework for isothermal multiphase multi-component problems. A more detailed description can be found in [14]–[16].

2.3.1 Parameterization of Sub-critical Problems

First, we consider the methodology for immiscible two-phase multi-component displacement problems. Suppose we know that the solution route is close to the tie-line passing through a given point in the compositional space (*base point*). We need to develop a strategy to represent compositions in the vicinity of the base point over the entire pressure range of the simulation. For this purpose, a discrete pressure grid is constructed and compositional space around the base point is represented at discrete pressure levels [14]. *Tabulation* of the tie-lines starts by calculating compositions of the tie-lines through the base point from a minimum user-defined pressure (p_{min}). Tie-lines are calculated at discrete pressure values until the maximum user-defined pressure (p_{max}), or the critical point is reached. The minimal p at which the length of the tie-line through the base point is close to zero is called the Minimal Critical Pressure (MCP), see figure (2.3).

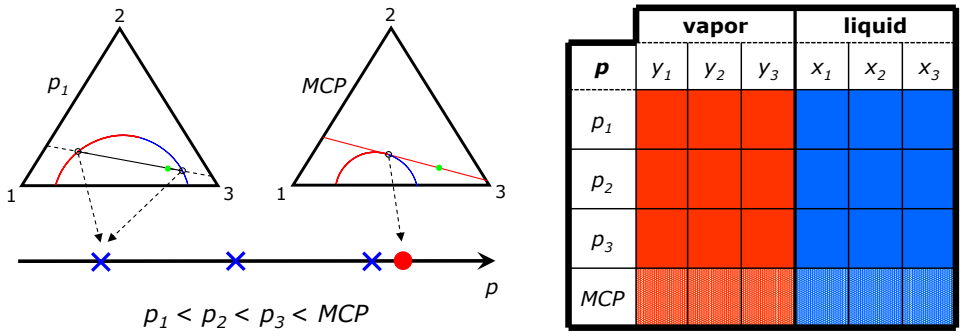

Figure 2.3: Calculation of tie-lines through a base point at different pressure levels with $N_p = 4$ (left); associated tie-line table (right)

A search scheme is employed to locate the MCP between two pressure values [16]. The tie-lines associated with the base point are stored using a uniform pressure grid:

$$(p_i)_{i\in\{0,N_p-1\}} = (p_{min} + i\Delta p) \qquad \text{with} \qquad \Delta p = \frac{p_{max} - p_{min}}{N_p - 1}, \tag{2.9}$$

where N_p is the number of discrete pressure values between p_{min} and p_{max}, inclusive.

Since the calculated tie-lines in the table are likely to be at pressure values different from the pressure of other composition points in the simulation (called *test points*), interpolation in pressure is performed in order to calculate a tie-line that is considered to be quite close to the test point. For this purpose, the appropriate pressure index (i) is obtained from:

$$0 < \frac{p - p_{min}}{\Delta p} - i < 1. \tag{2.10}$$

For $\forall p \in [p_i, p_{i+1}]$:

$$\delta p = \frac{p - p_i}{p_{i+1} - p_i}, \tag{2.11}$$

$$\bar{\chi}_p = \chi_{p_i} + \delta p(\chi_{p_{i+1}} - \chi_{p_i}), \tag{2.12}$$

where χ represents $\mathbf{x}$ and $\mathbf{y}$.

Once interpolated tie-line compositions $(\bar{\mathbf{x}}, \bar{\mathbf{y}})$ are calculated, the following relation is used to measure the 'distance' between the tie-line and the test point ($\mathbf{z}$):

$$\sqrt{\sum_{i=1}^{n_c}(z_i - \bar{x}_i L - \bar{y}_i(1-L))^2} < \varepsilon \qquad \text{where} \qquad L = \frac{z_k - \bar{y}_k}{\bar{x}_k - \bar{y}_k}. \tag{2.13}$$

If the point is close to the interpolated tie-line within a tolerance, then it belongs to the family of test points parameterized by that base point. Information from the tie-line (such as equilibrium phase compositions and phase state) are then used to precondition standard EoS calculations. On the other hand, if it is found that the point is far from the interpolated tie-line, it is used as a base point to construct a new table of tie-lines. Hence, the method is adaptive in terms of choosing base points. Moreover, regardless of the type of the compositional simulation, or the tolerance used in (2.13), the number of calculated tie-line tables is finite [14]. In gas injection problems, for example, candidate base points include compositions at, or around, the injection and initial conditions. This procedure is summarized in the following flowchart:

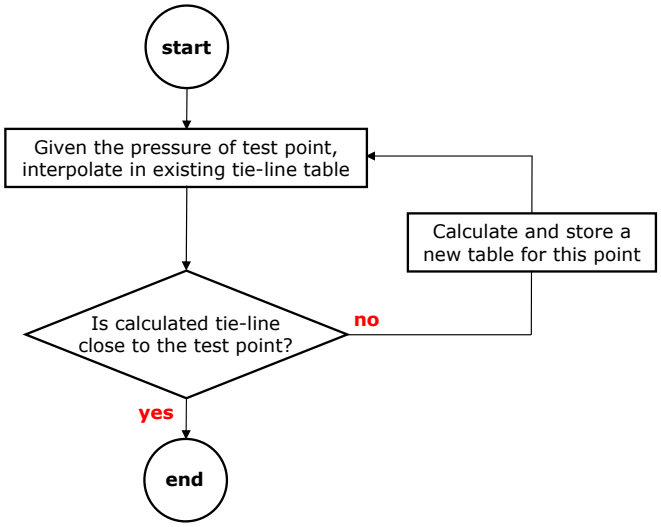

Figure 2.4: Table look-up and adaptive construction strategy for sub-critical compositions

Near-critical Representation

The algorithm described above works fine as long as the solution path is below the *MCP*. However, in compositional problems of practical interest, parts of the composition path lie in the super-critical region. Parameterization of the super-critical space is a challenging problem and will be discussed separately. Here, we consider the portion of the sub-critical space close to the critical locus.

Since the length of the tie-lines tends to zero as the pressure gets closer to the *MCP* (Minimum Critical Pressure) of the mixture, interpolation using tie-line tables with large pressure intervals (coarse discretization) can lead to poor approximation of the phase behavior. In order to resolve this issue, a refined table with small pressure intervals is constructed for the region just below the *MCP*, and it is linked to the corresponding coarse table [14]. Pressure intervals of the refined table decrease logarithmically as the pressure approaches the *MCP*:

$$(p_i)_{i\in\{1,10\}} \quad = \quad (MCP + (\log i - 1)\Delta p_{refined}), \tag{2.14}$$

where $\Delta p_{refined}$ defines the support of the refined table. This tabulation improves the quality of interpolation in the near-critical region quite significantly. Figure (2.5) shows the structure of an isothermal tie-line table containing both coarse and refined tables. The interpolation procedure in the refined table is similar to that used for the coarse table.

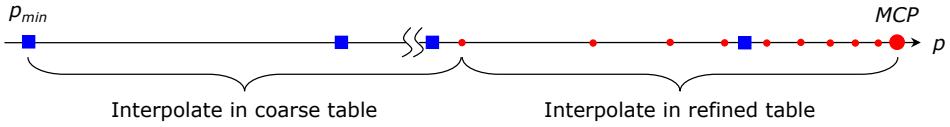

Figure 2.5: Tie-lines in coarse table (blue squares) and in refined table (red circles) for an isothermal tie-line table

2.3.2 Parameterization of the Super-critical Region

While parameterization of the sub-critical space is quite important for general-purpose compositional simulation, accurate representation of the super-critical space is essential for dealing with practical gas injection processes. The challenge is the fact that tie-lines do not exist in the super-critical space. To deal with this problem, the critical surface of the system can be pre-computed and stored at discrete pressure values before the simulation. The location of a composition with respect to the critical surface (sub- or super-critical) can be determined from a simple geometrical test [15]. If the composition is identified as super-critical, standard correlations are used to identify the state as vapor– or liquid–like [17].

This strategy, which we refer to as the Super-critical State Criteria (SSC) leads to a number of difficulties for general–purpose compositional simulation [16]. First, accurate and efficient pre-computation of the critical surfaces becomes an issue as the number of components increases. Moreover, interpolation of the critical surface in terms of pressure may lead to poor results, which could yield wrong identification of the phase state. In order

to overcome these difficulties, an adaptive SSC approach has been designed, where critical tie-lines are calculated and stored as needed in the course of simulation [16].

The main idea is to note that a unique critical tie-line passes through each point in the compositional space at fixed T (See figure 2.6). This is because the critical tie-line is the limiting tie-line among all lines that parameterize the space at fixed pressure and temperature. Considering that sub-critical tie-lines uniquely parameterize the sub-critical space, the associated critical tie-line also uniquely parameterizes a line of compositions. As a result, the entire space (at constant T) is parameterized by critical tie-lines with different *MCP*s (See figure 2.6).

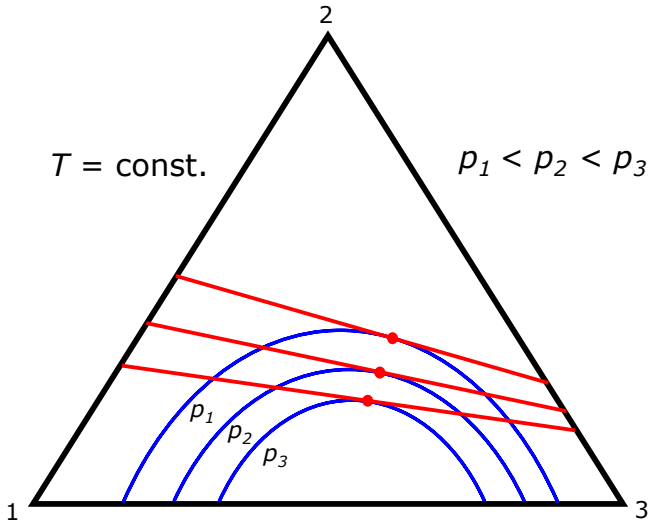

Figure 2.6: Space parameterization using critical tie-lines

As discussed before, during the calculation of a tie-line table, critical tie-lines are computed when the user-defined p_{max} is large enough to accommodate the *MCP*. This is an indication that there are compositions above the critical region. Noting that critical tie-lines parameterize the entire compositional space, calculated critical tie-lines are intersected with

test points. No interpolation in pressure is required, since the pressure of the critical tie-line through a base point is unique at fixed T. The intersection is accepted within a tolerance (2.13). If the test point is already parameterized by a critical tie-line, the corresponding pressures are compared. If the pressure of the test point is smaller, it is either in the sub-critical space, or a new critical tie-line should be calculated. Whereas, if the pressure of the test point is larger, the composition is super-critical. Similar to interpolation in sub-critical space, information from the interpolation is used to determine the phase state of the composition [16]. Figure (2.7) shows the flowchart for this Super-critical State Criteria (SSC).

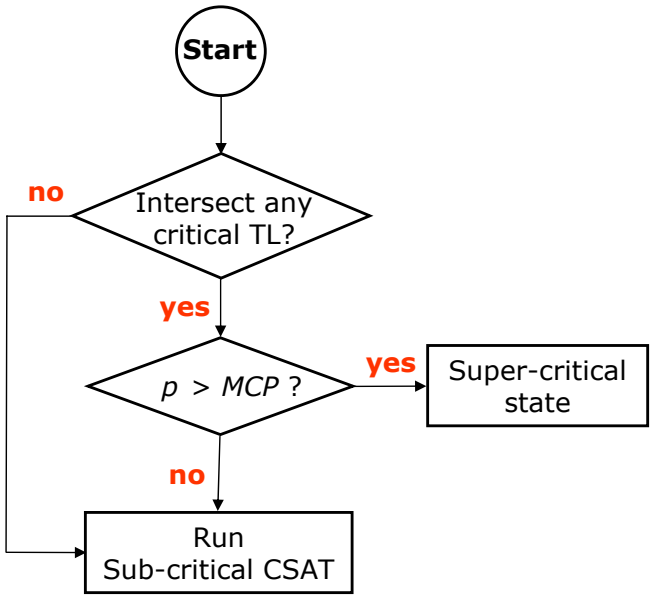

Figure 2.7: Adaptive Super-critical State Criteria (SSC)

2.3.3 Combining Super-critical State Criteria with Sub-critical State Parameterization

So far, we have considered the details of parameterization of the sub-critical and super-critical spaces. These parameterizations are combined to construct a general-purpose algorithm for isothermal multi-contact miscible displacements [15].

Given a test (composition) point, it is first checked in the table of critical tie-lines to identify its location in the space relative to the critical surface. This test determines if the point belongs to the super-critical state, or the sub-critical region. In the second case, based on the pressure of the test point, it is located in the existing tables of tie-line. A pressure larger than the *MCP* of the table indicates that the point can not be parameterized using the current table. Otherwise, interpolation in a regular or refined table identifies the thermodynamic state of the test point. Finally, if sub-critical state identification fails, the compositional space is tabulated for this point, and the resulting tie-line table is added to the existing list.

2.4 Tie-Line Parameterization of Thermal Problems

When energy conservation is also considered along with the system of flow and transport equations, treatment of the thermodynamic phase behavior becomes more complicated due to changes in both p and T . Therefore, a parameterization methodology should simultaneously account for p and T. Considering the fact that pressure and temperature are independent variables in computing two-phase binodal surface, we use them as our primary variables for tie-line tabulation and interpolation.

In the following section, we first generalize the isothermal parameterization methodology to thermal immiscible displacements. Then, after considering first contact miscible

problems, we combine the two schemes to obtain a general-purpose methodology.

In the next chapter, we will show that when both temperature and pressure vary along the composition path, single-phase compositions on the path are close to a limited number of tie-lines. This suggests parameterization of the compositional space along a single base point over the interval of p and T. Other test points are checked to see if they intersect an existing tie-line. This is the basic idea of adaptive space tabulation described in the following section.

2.4.1 Parameterization of Sub-critical Thermal Problems

The parameterization techniques of isothermal compositional simulation [14] can be generalized for thermal problems. Upper and lower bounds for pressure and temperature as well as the number of discretization points in both variables are determined by the user. This information defines the coarse $p-T$ grid over which tie-lines through the test point are computed:

$$\Delta p = \frac{p_{max}-p_{min}}{N_p-1}, \tag{2.15}$$

$$\Delta T = \frac{T_{max}-T_{min}}{N_T-1}, \tag{2.16}$$

$$(p_i,T_j)_{i\in\{0,N_p-1\};\,j\in\{0,N_T-1\}} = (p_{min}+i\Delta p, T_{min}+j\Delta T). \tag{2.17}$$

At each temperature value and starting from p_{min}, tie-lines through the base point are calculated at discrete pressure values until either the MCP (for current T), or the maximum allowable pressure (p_{max}), is reached. Following the same procedure for all discrete temperature values, the coarse table for the base composition point is generated. Depending on the values of MCP_j and p_{max}, each temperature value may, or may not, contain the MCP, and this information is used to control the structure of both the coarse and refined tables.

Since the p and T of the compositions (test points) encountered in the course of a

simulation are expected to be different from the discrete pressure and temperature levels of the $p-T$ grid, interpolation is required to obtain the closest approximation of the tie-line through a test point. The pressure index for a given test point is obtained from (2.10). Similarly, the appropriate temperature index (j) satisfies:

$$0 < \frac{T - T_{min}}{\Delta T} - j < 1. \tag{2.18}$$

For $\forall (p,T) \in ([p_i, p_{i+1}], [T_j, T_{j+1}])$, bilinear interpolation in p and T is used to determine tie-line equilibrium compositions:

$$\delta p = \frac{p - p_i}{p_{i+1} - p_i}, \tag{2.19}$$

$$\delta T = \frac{T - T_j}{T_{j+1} - T_j}, \tag{2.20}$$

$$\chi_{p,T_{j,j+1}} = \chi_{p_i,T_{j,j+1}} + \delta p(\chi_{p_{i+1}} - \chi_{p_i})_{T_{j,j+1}}, \tag{2.21}$$

$$\bar{\chi}_{p,T} = \chi_{p,T_j} + \delta T(\chi_{T_{j+1}} - \chi_{T_j})_p, \tag{2.22}$$

where χ represents $\mathbf{x}$ or $\mathbf{y}$. Although standard EoS computations involve the solution of highly nonlinear systems of equations; the overall structure of the two-phase binodal surface does not change significantly if the pressure and temperature variations are small. Therefore, the bilinear interpolation described above is well behaved and provides a reasonable representation.

The interpolated tie-line is not identical to the actual tie-line through the test point and is acceptable only if it is close to the test composition within a tolerance. The same criteria in (2.13) is used to verify the accuracy of the bilinear interpolation. If it is found that the test point is 'far' from the interpolated tie-line, a new tie-line table is generated.

Near-critical Representation over $p-T$ Grid

Parameterizing compositional space at pressure and temperature values just below the *MCP* loci is more challenging. This is because two nearby discrete temperature values

have distinct *MCP*s. Due to this fact, the bilinear interpolation technique introduced in the previous section is not applicable. Moreover, thermodynamic behavior of two phases becomes identical when $p - T$ conditions are close to the critical loci. Since a majority of important thermal compositional problems have solution paths in the neighborhood of the critical surface, an effective and general interpretation of the near-critical region is required.

Due to the fact that the length of tie-lines tends to zero in the near-critical region, coarse tie-line tabulation is not effective, and a refined tabulation procedure is used. For temperature values, which contain a critical point, another table of tie-lines over a refined p grid just below the *MCP* is calculated. This is the same procedure used for isothermal problems. (2.14) Obviously, a refined table is not generated for T values that do not have an *MCP*. Figure (2.8) summarizes the table structures obtained using this methodology.

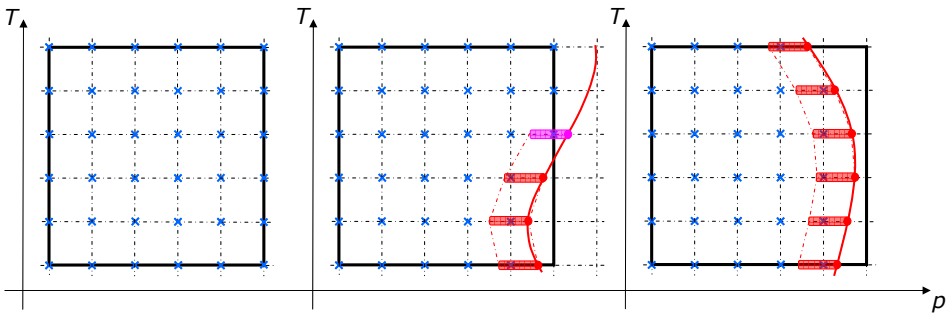

Figure 2.8: Generic tie-line table structure on $p - T$ grid, none of the temperature values (left), some of them (center) or all of them (right) contain an MCP. Note the construction of the additional refined table in the second case. Pressure and temperature bounds are defined by the black frame.

In order to define the range of support for interpolation, an estimate of the *MCP* for a given temperature is needed. We use linear interpolation in temperature for this purpose.

For $\forall T \in [T_j, T_{j+1}]$:

$$\overline{MCP} \quad = \quad MCP_{T_j} + \delta T(MCP_{T_{j+1}} - MCP_{T_j}), \tag{2.23}$$

where δT is defined in (2.20) and j is given by (2.18). Pressure values above the interpolated MCP belong to the super-critical space and cannot be parameterized using the existing table.

A different interpolation technique is employed for the near-critical region. Noting that the tie-line length is zero at MCP, and that the tie-line length increases gradually as one moves away from the MCP, we assume that the behavior of the tie-line length is similar to those at nearby temperature points. Therefore, we can interpolate in terms of the 'length' of tie-lines. For this purpose, tie-lines with identical pressure indices from two refined tables (associated with nearby temperature values) are used for bilinear interpolation. The pressure index ($\hat{i}$) is chosen such that:

$$\log \hat{i} < \frac{p + \Delta p_{refined} - \overline{MCP}}{\Delta p_{refined}} < \log (\hat{i} + 1). \tag{2.24}$$

Using $\hat{i}$ instead of i in equations 2.19 to 2.22, a modified bilinear interpolation in p and T is performed. This idea is shown in figure 2.9:

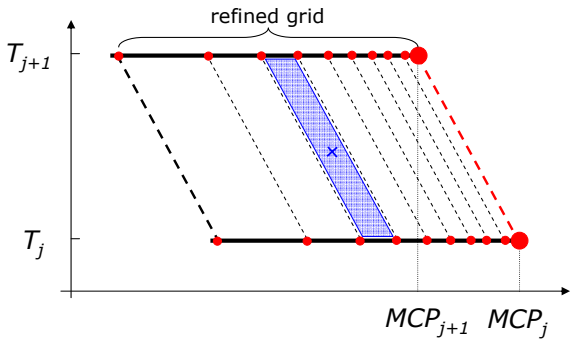

Figure 2.9: Refined interpolation, four tie-lines at the corners of the parallelogram are used for interpolation

2.4.2 Parameterization of Super-critical Thermal Problem

Since in the framework of compositional space parameterization, the effect of T can be treated much like the effect of p, extension of isothermal SSC to thermal problems is straightforward. The compositional space at fixed T is parameterized by a set of critical tie-lines, and interpolation in T is required before intersection with a test point:

$$\bar{\chi}_{cr} = \chi_{cr,T_j} + \delta T(\chi_{cr,T_{j+1}} - \chi_{cr,T_j}), \tag{2.25}$$

where critical compositions are represented by χ_{cr}. The *MCP* associated with this interpolated critical tie-line is computed from (2.23). After performing the temperature interpolation defined by (2.25), the problem becomes 'isothermal' and therefore, an algorithm similar to that for isothermal SSC (figure 2.7) can be used.

2.4.3 Parameterization for General-purpose Thermal Compositional Simulation

An effective tie-line based interpolation framework has been developed to parameterize general thermal compositional problems. A composition is first checked in the table of critical tie-lines to identify its location relative to the critical surface. When the point needs to be checked in the sub-critical table, various strategies are employed to ensure that the best interpolation results are obtained. In this section, we summarize this framework.

Considering the fact that both coarse and refined tables are constructed for the near-critical region, one should first choose which table will be used for bilinear interpolation. For $p-T$ conditions, which have a refined table of tie-lines on one T side and a coarse table on the other side, a 'mixed' interpolation in both tables is employed. Figure (2.10) shows schematic of two tie-line tables at temperatures T_j and T_{j+1}. Note that in the neighborhood of an *MCP*, a refined table is constructed. For a given composition at $T \in [T_j, T_{j+1}]$, we compute the *MCP* by interpolating between the two *MCP*s. For every composition at

that temperature, we can use the appropriate coarse and/or refined tables for interpolation.

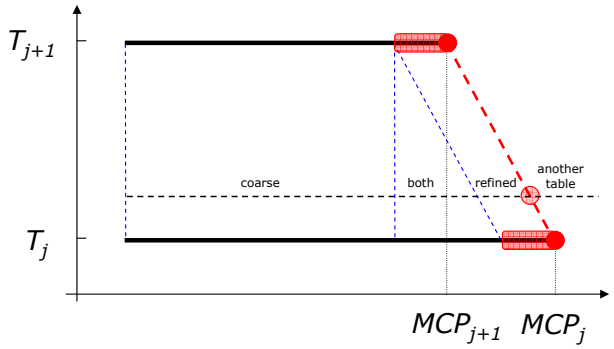

Figure 2.10: Sub-critical interpolation framework, test point could be anywhere along the horizontal dashed line

Note that if the separation in the temperature values is large, or support of the refined table is small, it is possible that neither table would give reasonable interpolation results. These issues can be resolved by modifying the user-input interpolation parameters.

The treatment in the near-critical region is performed only when two adjacent temperature values are associated with a critical tie-line and *MCP*. Otherwise, interpolation using the coarse table is performed.

Chapter 3

Implementation and Numerical Results

In this Chapter, we discuss the implementation of the Compositional Space Adaptive Tabulation (CSAT) method in a general–purpose thermal–compositional research simulator. A variety of numerical examples are then presented to illustrate the accuracy and efficiency of CSAT for challenging thermal compositional problems.

3.1 Implementation

CSAT for isothermal problems has been implemented in a general-purpose research simulator [22], [14]–[16]. In this section, we briefly review how the algorithms introduced previously are extended for thermal problems.

3.1.1 Tie-line Table Construction

Given p_{min}, p_{max} and N_p, the coarse pressure grid for a temperature value is defined by (2.9). Calculation of tie-lines starts from p_{min} at discrete pressure levels until p_{max} is reached, or flash calculations converge to a trivial solution, which indicates the pressure has

passed the *MCP* (See algorithm 3.1).

```
for each T value (T_j)
  for each p value (p_i)
  {
      // provide initial guess for K-values
      if (i == 0)
          Get K-values from Wilson's correlation;
      else
          Use K-values from (i-1) and (j);
      Compute TL for z, p_i and T_j; // using standard EoS module
      if (trivial TL)
          Compute MCP for T_j;
          break;
  }
```

Algorithm 3.1: Pseudo-code for generating tie-line table

For the second case, the *MCP* associated with the temperature value should be computed. By definition, the *MCP* is the pressure value at which the length of the tie-line through a base point is close to zero. The corresponding critical tie-line is defined such that its length is bounded by two small values:

$$\varepsilon_{min} < \ell_{tie\text{-}line} \equiv \sqrt{\sum_i (x_i - y_i)^2} < \varepsilon_{max}. \tag{3.1}$$

This criterion is satisfied by a range of pressures (See figure 3.1). Noting that the *MCP* lies

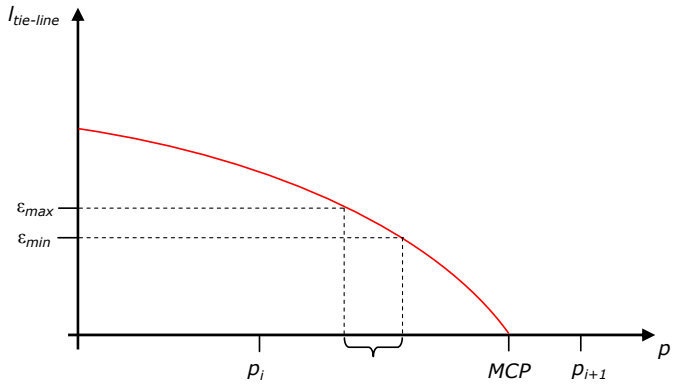

Figure 3.1: Variation of tie-line length in the near-critical region, the binary search returns a result bounded by the curly bracket

somewhere between pressure levels p_i and p_{i+1}, a binary search scheme is used:

```
p1 = pi; p2 = pi+1;
while (true)
{
  MCP = 0.5*(p1+p2);
  Compute TL at MCP and Tj;
  if (lTL > εmax)
      p1 = MCP;
  else if (lTL < εmin)
      p2 = MCP;
  else
      return MCP;
}
```

Algorithm 3.2: Pseudo-code for computing MCP

Calculation of the *MCP* is followed by constructing a refined table for the temperature value. A similar procedure to the pressure treatment of algorithm(3.1) is employed. Here, the pressure grid is defined by (2.14) for given $\Delta p_{refined}$. Calculation of near-critical tie-lines starts from the lowest p in the refined table using K-values from nearby existing tie-lines.

At this point, tie-lines (with the associated critical tie-line, if it exists) have been computed for each temperature level. Next, the tables should be further processed to become consistent with the interpolation schemes. We make sure that if an *MCP* has been calculated for temperature value T_j, both T_{j-1} and T_{j+1} must also be supported by a refined table. This ensures that the general interpolation technique will cover all temperature values between any T_j and T_{j-1} or T_{j+1} properly.

Calling `PostProcessTable(0)` presented in algorithm (3.3), performs this task. This function uses flags of `isCrit` to check if each temperature value has been assigned an *MCP* during the tie-line table construction procedure, or not. When necessary, the function computes the *MCP* and updates the refined table.

```
void PostProcessTable(j)
{
  if (N_T > 1)                          // thermal
      if (j == N_T-1)                   // terminate recursion
          if (isCrit_{N_T-2})
              Compute MCP;
          return;
      else if (j == 0 && isCrit_1 || j != 0 && (isCrit_{j-1} || isCrit_{j+1}))
          Compute MCP;
      PostProcessTable(j+1);
}
```

Algorithm 3.3: Post-process of table of tie-lines

The critical tie-lines computed during the construction of a coarse table (if any) are collected in the critical tie-line table, which parameterizes the critical surface along a particular base point. This completes the construction of tie-line tables through a base point.

3.1.2 Critical Tie-line Table Check

Before determining a suitable methodology for given compositions, its state in the compositional space with respect to the critical surface should be determined. For this purpose, compositions are first checked in the table of critical tie-lines, which were adaptively collected in the course of simulation.

Using the temperature index obtained from (2.18), interpolation in the critical tie-line table is performed if both nearby temperature levels contain a critical point (Algorithm 3.4).

```
for all critical tie-line tables
{
  if (hasMCP_{j-1} && hasMCP_j)
      Interpolate using (2.23) and (2.25);
      if intersects test point && (p > MCP)
          Super-critical, Return from CSAT;
}
```

Algorithm 3.4: Pseudo-code for Super-critical State Criteria

Check in the table of critical tie-lines is performed in the first level a composition is passed to the procedure. Therefore, if T_j and T_{j-1} are both in the sub-critical state, the

methodology skips the current table.

3.1.3 Sub-critical Tie-line Check

Following the same procedure discussed in the previous chapter, a given point is first located in the tie-line table by finding its temperature index using (2.18). Afterwards, based on the pressure of the point, an appropriate interpolation scheme is applied (See algorithm 3.5). Interpolation using coarse and refined tables follows (2.22) with suitable pressure indices determined by (2.10) or (2.24). If the interpolation yields a tie-line that is far from the test point, a new table of tie-lines is calculated (See algorithms 3.1–3.3). Algorithm (3.6) summarizes the general structure for fully adaptive thermal CSAT.

```
for all tables of sub-critical tie-lines
{
  if (hasMCP_{j-1} && hasMCP_j)
      Let MCP_min = min(MCP_{j-1}, MCP_j);
      Get MCP-bar from (2.23);
      if (MCP-bar < p)
          Next table;
      else if (MCP-bar − Δp_refined < p < MCP-bar)
          Interpolate in refined table;
      else if (MCP_min < p < MCP-bar − Δp_refined)
          No support, Increase Δp_refined or N_T;
      else if (MCP_min − Δp_refined < p < MCP_min)
          Interpolate in both tables;
  Interpolate in coarse table;
}
```

Algorithm 3.5: Pseudo-code for sub-critical tie-line table check

```
CSAT(.)
{
  if !algorithm(3.4)
      if !algorithm(3.5)
          if algorithm(3.1)     // which may call algorithms(3.2) and (3.3)
              CSAT(.);          // call CSAT for the base point itself
  Run standard EoS module;      // CSAT failure
}
```

Algorithm 3.6: CSAT control structure

3.2 Numerical Examples

Isothermal CSAT, Application to a Field Problem

The initial implementation of CSAT for isothermal compositional problems has been tested on a field problem. In this section, we present performance studies of CSAT for the simulation of important recovery scenarios for large-scale problems.

Figure (3.2) shows a layout of the model used to test the isothermal CSAT algorithm. The fractured system is modeled using over a thousand discrete fractures [23]. From more than 200000 tetrahedral grid blocks of this model, almost 20% are in the fractures. The compositional fluid is represented using six components. First contact miscible gas injection and depletion below the bubble–point pressure are considered in the presence of gravity effects.

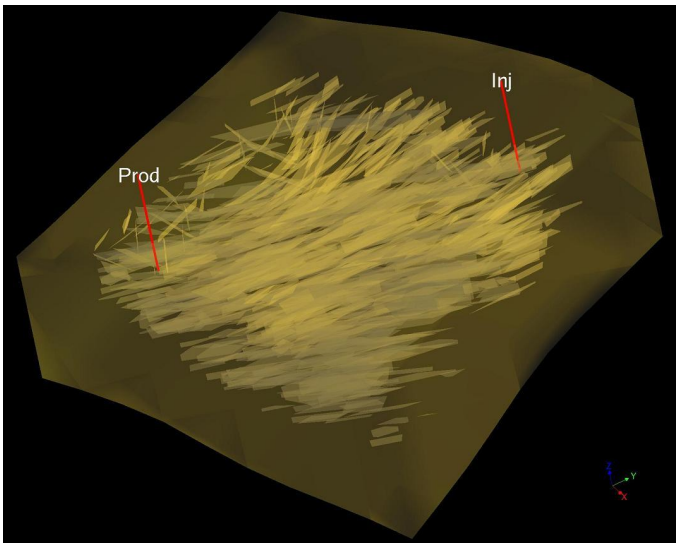

Figure 3.2: Fracture network of the model used for case studies

Table (3.1) represents performance results for the depletion simulation of this model at

pressures below the bubble point. Since variation in the composition of the cells during simulation is relatively small for the depletion problem, parameterization of the compositional space around a limited number of composition points increases the efficiency of the simulation significantly. As indicated by table (3.1), with almost the same number of Newton iterations, EoS time for CSAT is orders of magnitude smaller than that of the standard approach. This effect is reflected in the total CPU time of the two simulations.

Table 3.1: CSAT efficiency for depletion below the bubble point, CPU time is reported in (hr:min)

Method	# Newton iterations	Solver time	EoS time	Total time
standard	3070	15:22	42:16	63:24
CSAT	2929	12:09	00:17	17:14

As another example, we study the applicability and efficiency of CSAT when the number of components used to represent the fluids increases. Here, we consider first contact miscible injection on a coarser representation of the same model used in the previous example (roughly 5000 cells). Table (3.2) summarizes the performance comparison of CSAT and standard methods. The computational gain in EoS time is more significant when the number of components is larger. A close examination of these results indicates that the speedup in terms of total CPU time is almost the same for the three scenarios. This is because increasing the number of components affects the solver portion of the fully implicit simulation significantly; as a result, EoS computations are no longer the most time-consuming component of the simulation. This argument is verified by observing that non-EoS time of standard and CSAT approaches are almost the same for all cases and that EoS time of CSAT is only a very small portion of total CPU time.

Table 3.2: Isothermal CSAT vs. standard approach: sensitivity to number of components, CPU time is reported in seconds

# of components	Method	EoS time	Total time	Speedup, EoS– Total
4	Standard	1 100	2 570	1–1
	CSAT	20	1 370	55–1.9
6	Standard	1 760	3 970	1–1
	CSAT	24	1 970	73–2.0
26	Standard	28 500	71 500	1–1
	CSAT	39	36 020	730–2.0

3.2.1 Thermal CSAT Accuracy, Case Study

As discussed previously, an important strength of tie-line based parameterization approach is that a compositional displacement problem normally takes place in a small portion of the compositional space [16]. Therefore, parameterization of the space along some base points at distinct pressure (and temperature) levels provides a reasonable representation of the phase behavior for the entire simulation [13, 14].

Thermodynamic phase behavior for the compositions of other cells in the problem (test points) are obtained using interpolation from nearby tie-lines. This interpolation in p and T is then used to precondition standard EoS calculations. In order to show the accuracy of this strategy, one should first show how close these interpolated results are to standard EoS computations. In this section, we study this question using a simple numerical experiment in the absence of hydrodynamic effects.

For this purpose, an 11-component mixture has been chosen [21, mixture III]. Table (3.3) shows the compositions and thermodynamic properties of this mixture. For this composition point, coarse and refined tables of tie-lines are constructed using the parameters summarized in table (3.4). These tables of tie-lines are then used to provide initial guess for

Table 3.3: Composition and properties of the test mixture [21]

Component	Mol. (%)	MW	$T_c(K)$	$P_c(bar)$	ω	$\delta_{C_1-C_i}$
C_1	81.107	16.04	190.6	45.4	0.008	0
C_2	3.914	30.07	305.4	48.2	0.098	0
C_3	1.958	44.1	369.8	41.9	0.152	0
C_4	1.628	58.12	419.6	37.0	0.187	0
C_5	1.105	72.15	448.8	33.3	0.243	0
C_6	1.197	84	506.35	33.9	0.299	0.01
C_{7-9}	2.73	107	554.13	29.7	0.428	0.01
C_{10-12}	2.2973	147	622.3	24.5	0.611	0.02
C_{13-15}	1.2491	190	679.0	20.3	0.776	0.02
C_{16-18}	0.8473	237	727.0	16.8	0.940	0.02
C_{19+}	1.9673	385.08	809.0	10.0	1.668	0

standard negative flash of the same composition point at $T = 650°\text{R}$ over the entire range of pressure. (via interpolation in both p and T)

Table 3.4: Tie-line table parameters

p range	1000–10000 $psia$
Δp_{coarse}	500 $psia$
$\Delta p_{refined}$	1000 $psia$
T range	640–660 °R
ΔT	20 °R

The quality of the initial guess is then compared with that obtained from standard approaches. Wilson's correlation [16] and phase stability tests [4] are used as standard procedures. The number of flash iterations is normalized in terms of N_{Newton} with $N_{SSI} \approx$

$0.7N_{Newton}$ is used to compare the performance of different flash procedures [21].

Figure(3.3) compares the number of normalized flash iterations for different approaches. While the numerical results obtained from all four methods are identical, a large difference in the quality of the initial guess is observed. The number of flash iterations is at least an order of magnitude larger when standard approaches are employed. The difference with standard methods becomes more evident for near-critical pressures. We observe that although the flash procedure suffers from poor standard initial guesses for these pressures, interpolation results obtained from the refined table of tie-lines are very close to the actual EoS computations.

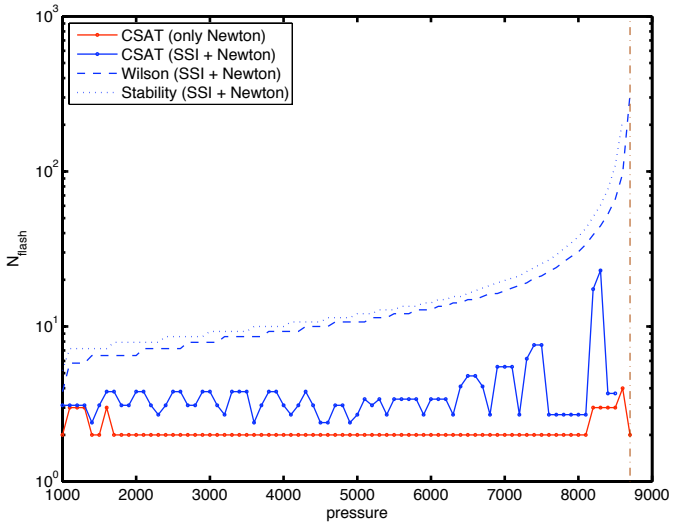

Figure 3.3: Negative flash with initial guess from space tabulation and standard procedures

Figure (3.3) also reflects the structure of the coarse table of tie-lines. The number of flash iterations decreases at pressure values close to those computed via (2.9). In fact, interpolation results from the table of tie-lines can be used directly in the Newton's method

to perform the flash (a procedure which requires a good initial guess). It should be noted that since space tabulation provides excellent performance in determining the super-critical state, the comparisons are made all the way up to the mixture's *MCP*.

Similar behavior is observed when the temperature of the system is changed (figure 3.4). Although the number of flash iterations for the standard method increases in the near-critical region, little sensitivity is observed from interpolation at different temperatures in the near-critical region.

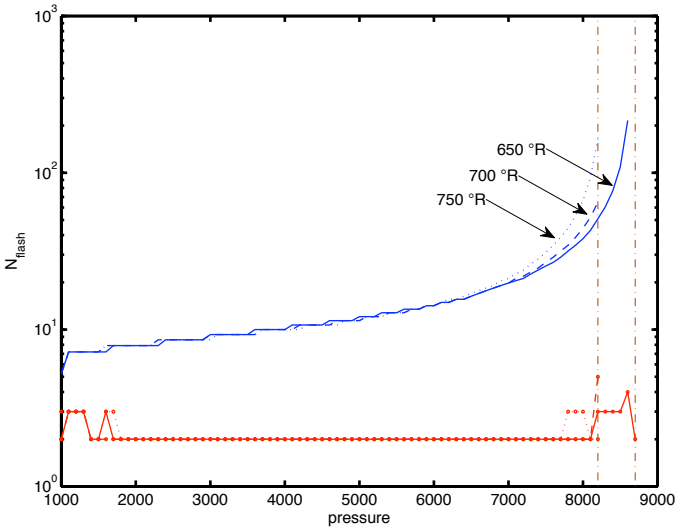

Figure 3.4: Negative flash with initial guess from space tabulation (red) and phase stability test (blue): sensitivity to temperature; Tables of tie-lines are computed at different temperatures

Sensitivity to the difference in temperature values of the table is also studied for the same mixture (figure 3.5). The results obtained from interpolation are almost indifferent to coarseness of the table of tie-lines in terms of temperature. This indicates that the general structure of the binodal surface changes almost linearly with temperature even when the number of components is large.

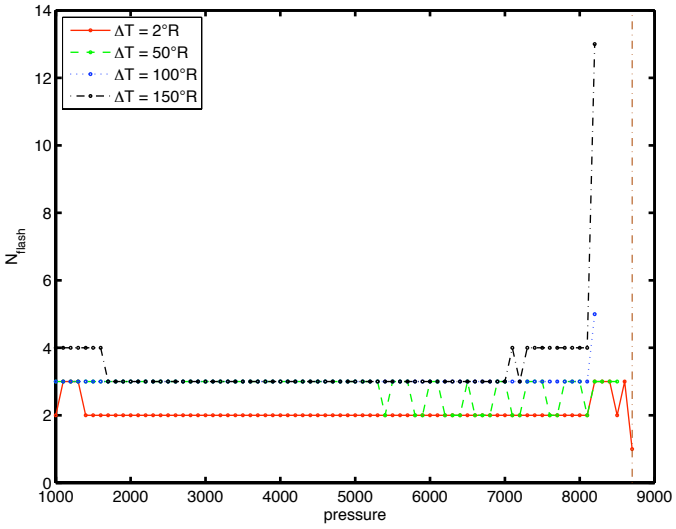

Figure 3.5: Space tabulation: sensitivity to coarseness in temperature tabulation

3.2.2 Thermal CSAT, Application to Compositional Flow Simulation

In this section, we present the results of some test cases in order to show the accuracy and efficiency of our approach. A general-purpose research simulator [22] has been used to test the implementation outlined in the previous sections. An extensive set of examples for isothermal implementation can be found in [14]–[16].

Base Case I, First Contact Miscible Displacement

The first example is the simulation of a first contact miscible displacement problem. A mixture of $\{C_1(20\%), CO_2(80\%)\}$ at 810°R is used to displace $\{C_1(20\%), CO_2(5\%), C_4(30\%)$ $, C_{10}(45\%)\}$ at a reservoir temperature of 710°R. An injector and a producer operate under BHP control of 3800 and 3200 $psia$, respectively. A one dimensional reservoir model with 100 cells is used where the injector and producer are at opposite ends of the model. Figure(3.6) shows the concentration profiles of the four components in the middle of the displacement as well as the solution route in compositional space. Binodal surfaces at reservoir and injection temperatures are plotted to observe interactions with the solution path. It should be noted

that both pressure and temperature change along the path.

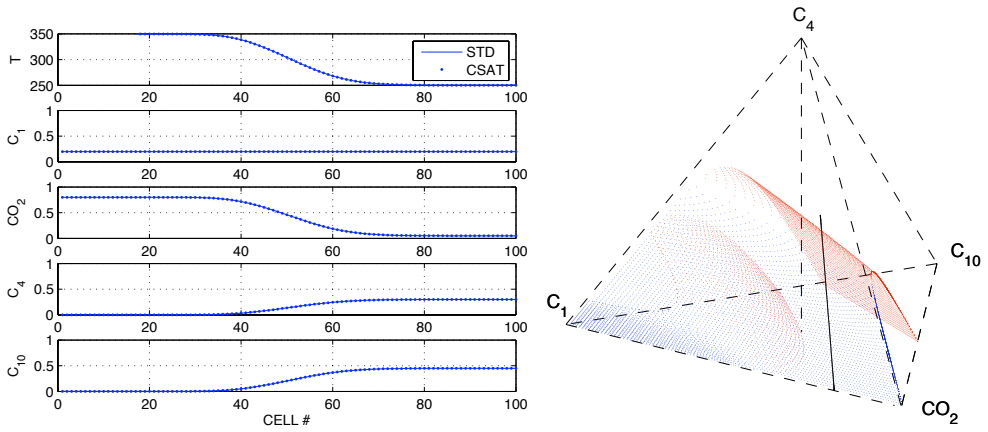

Figure 3.6: Base case I: temperature and composition profiles (left), solution path in compositional space(right) with binodal surfaces at initial and injection conditions

The solution indicates a continuous variation in compositions (caused by physical transport and numerical dispersion) along the route between the injector and producer, and that the path is mainly in the super-critical space.

Base Case II, Multi-contact Miscible Displacement

The second base case verifies the accuracy of the implementation for a multi-contact miscible displacement. Changing the initial and injection compositions of case I leads to a solution path, which is partly in the super-critical space and partly in the subcritical region (figure 3.7). Similar to the isothermal CSAT examples in [16], the solution path crosses the critical surface, but here, these surfaces are at different temperatures.

A comparison of CSAT results with those of the standard approach indicates a perfect match between the two methods. This is what one expects since CSAT is used as a preconditioner for standard EoS computations.

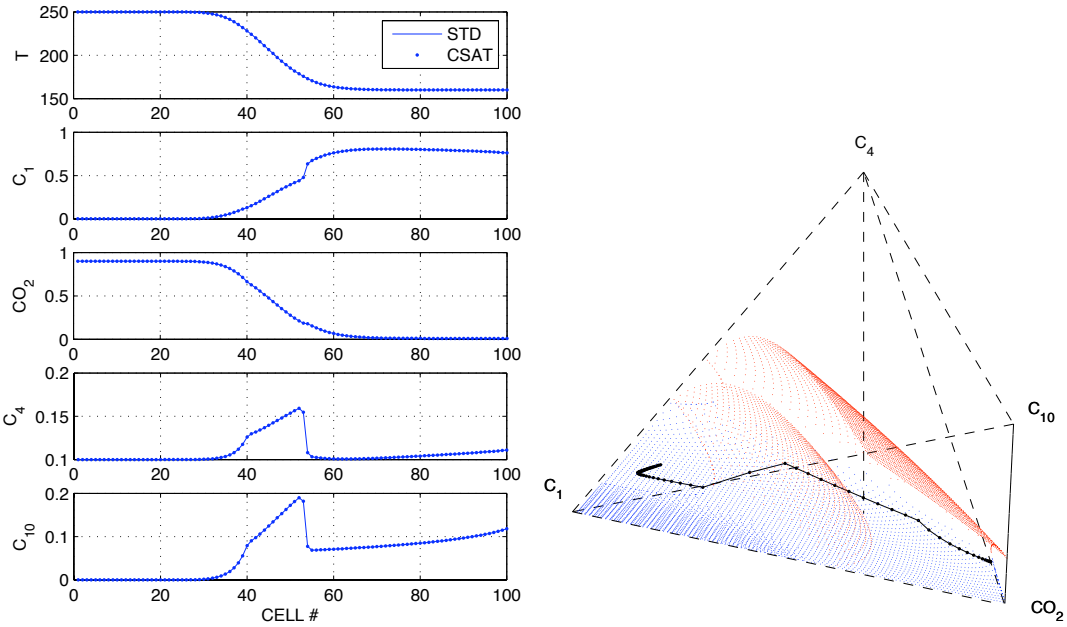

Figure 3.7: Base case II: temperature and composition profiles (left), solution path (right)

Standard Tests: SPE3 and SPE5

We demonstrate the applicability of thermal CSAT to standard tests using two SPE compositional problems: SPE3 and SPE5 [24, 25]. The first test has been modified to a thermal gas injection problem. For this purpose, a mixture of $\{C_1(70\%),C_2(30\%)\}$ at 650°R is injected into standard initial oil at 530°R. The injector and producer are at opposite corners of the model operating under BHP constraints of 4000 and 2000 *psia*, respectively.

For SPE5, five periods of water at 620°R and gas $\{C_1(77\%), C_3(20\%), C_6(3\%)\}$ at 600°R are injected into standard oil composition at 520°R. The injector and producer operate at 5000 and 3000 *psia*, respectively.

We study the impact of grid size on the efficiency of thermal CSAT over conventional

approach. Simulations are performed by refining the horizontal layers of the model. A rough idea about the distribution of the simulation composition points over the $p-T$ grid can be obtained from table (3.5), which shows the dominant interpolation routines in the simulation. For SPE3, almost 80% of compositions are identified via interpolation using critical surface. The remaining compositions lie along extensions of sub-critical tie-lines (figure 3.6). However, for SPE5, the compositions are essentially in the subcritical space.

Table 3.5: Calls (x10^5) to various interpolation routines of thermal CSAT for SPE3 (top) and SPE5 (bottom); values in parentheses indicate the percentage of positive identification based on (2.13) from the total calls to the routine. Since the critical check is performed in the first level, summation of all positive identifications equals the total calls to the critical check tests.

Grid size	Critical check	Non-critical table	Refined table	Both tables	Coarse table
15x15x5	24.2 (79.2%)	4.3 (91.5%)	2.3 (49.5%)	0.12 (0.17%)	0.6 (0.01%)
20x20x5	52.4 (79.2%)	8.6 (82.8%)	0.005 (84.2%)	0.002 (26.1%)	9.4 (39.9%)
25x25x5	105.3 (80.7%)	31.0 (65.4%)	0.005 (100%)	0	0
14x14x3	23.5 (21.2%)	18.5 (95.9%)	0.37 (100%)	0.03 (100%)	0.35 (100%)
21x21x3	80.4 (19.6%)	64.6 (95.4%)	2.9 (100%)	0	0
28x28x3	207.4 (18.8%)	168.4 (96.8%)	4.3 (99.9%)	0.2 (100%)	0.9 (100%)

These examples demonstrate the robustness of thermal CSAT for the entire compositional space, since the encountered compositions exist in both super– and sub–critical spaces as well as the near-critical region. As a result, application of CSAT reduces the cost of phase stability tests during simulation (table 3.6), and leads to orders of magnitude speedup in the EoS portion of the computations (figure 3.8).

Table 3.6: Ratio (standard/CSAT) of SSI and Newton stability tests for SPE3 and SPE5

Run #	SPE3	SPE5
1	858–189	513–374
2	1152–263	1144–829
3	1574–367	1950–859

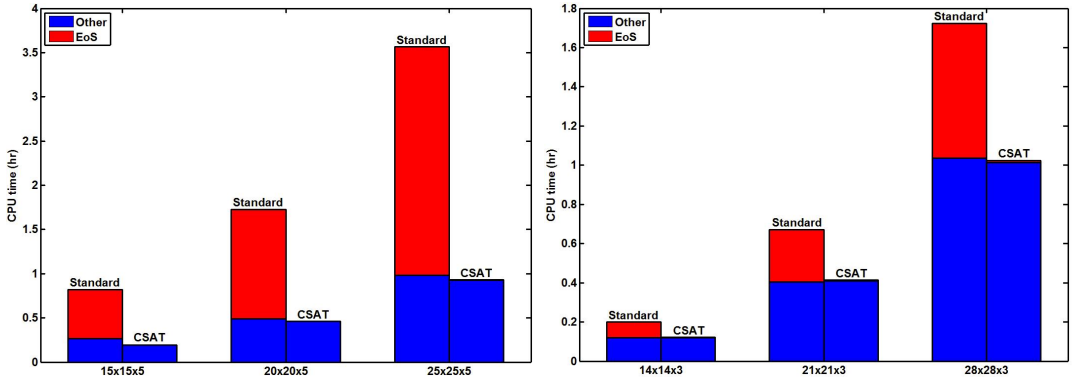

Figure 3.8: Thermal CSAT performance for SPE3 (left) and SPE5 (right), EoS time for CSAT based simulations is a weak function of grid size

Chapter 4

Conclusions

The applicability and effectiveness of the compositional space adaptive tabulation (CSAT) method for isothermal compositional reservoir simulation have been validated using field-scale compositional problems. We described the extension of this tie-line based parameterization framework to thermal–compositional problems. The accuracy and efficiency of our general-purpose approach have been demonstrated using a number of challenging test problems. The CSAT framework yields very accurate treatment of the entire compositional space and is orders of magnitude faster than standard approaches in terms of EoS (Equation of State) time, which is the dominant time-consuming kernel of standard compositional simulation. With CSAT, our results indicate that even for challenging compositional problems with large numbers of components, the EoS computational cost is a small fraction of the total time.

Different techniques are used to parameterize immiscible and multi-contact miscible displacements. The proposed approach for parameterization of the sub-critical space is motivated by theoretical findings from method-of-characteristics solutions of ideal problems, where tie-lines play a key role in the solution construction. In our approach, tie-lines are used to parameterize the phase behavior, and pressure interpolation in this tie-line space

is employed. The approach is effective in the presence of a wide range of complexities in immiscible gas injection simulations.

A critical surface is constructed and used to identify if a composition is sub– or super–critical at the prevailing pressure and temperature conditions. If a composition is sub–critical, tie–line parameterization is used. If the composition is super–critical, interpolation in critical tie–lines is used to identify if the phase is liquid–like or gas–like. The idea of parameterizing the critical surface has been extended to thermal problems, and we show that pressure and temperature effects can be handled in a robust and efficient manner in our CSAT framework.

We continue to explore more general and challenging physics (e.g, the presence of three or more phases) in the framework of compositional space parameterization. Based on the ideas of Γ-space parameterization [8, 10], one can decouple and discretize the thermodynamic part of general compositional flows in terms of tie-line variables. The insight obtained from this innovative approach allows for a fundamental understanding of the workings of various compositional displacement processes in large-scale reservoirs.

Bibliography

[1] Wang, Y.: *Analytical Calculation of Minimum Miscibility Pressure*, PhD Dissertation, Stanford University, Stanford, CA, (1998).

[2] Jessen, K.: *Effective Algorithms for the Study of Miscible Gas Injection Processes*, PhD Dissertation, Technical University of Denmark, Lyngby, Denmark (2000).

[3] Jessen, K., Michelsen, M.L., and Stenby, E.H.: "Global Approach for Calculation of Minimum Miscibility Pressure", *Fluid Phase Equilibria* (1998) **153**, 251-263.

[4] Firoozabadi, A.: *Thermodynamics of Hydrocarbon Reservoirs*, McGraw-Hill, New York, NY (1999).

[5] Michelsen, M.L. and Mollerup, J.M.: *Thermodynamic Models: Fundamentals and Computational Aspects*, Tie-line Publications, Holte, Denmark (2004).

[6] Johansen, T., Dindoruk, B., and Orr, F.M., Jr.: "Global Triangular Structure in Four-Component Conservation Laws", June (1994) Fourth European Conference on the Mathematics of Oil Recovery, Roros, Norway.

[7] Orr, F.M., Jr.: *Theory of Gas Injection Processes*, Tie-Line Publications, Copenhagen, Denmark (2007).

[8] Entov, V.M.: "Nonlinear Waves in Physicochemical Hydrodynamics of Enhanced Oil Recovery. Multicomponent Flows", Proceedings of the International Conference "Porous Media: Physics, Models, Simulations", Moscow, Russia, 19-21 Nov., (1997).

[9] Entov, V.M., and Voskov, D.V.: "On Oil Displacement by Gas Injection", Seventh European Conference on the Mathematics of Oil Recovery, Baveno, Italy, 5-8 Sep., (2000).

[10] Entov, V.M., and Voskov, D.V.: "On Oil Displacement by Gas Injection", Izv Ross. AN, Mekh. Zhidk. i Gaza, (2001), N2.

[11] Entov, V.M., and Voskov, D.V.: "Problem of Oil Displacement by Gas Mixtures", *Fluid Dynamics*, (2001) **36**, No. 2, 269-278.

[12] Voskov, D.V.: *Two-phase Multicomponent Flows Through Porous Media*, PhD thesis, Gubkin Russian State Oil and Gas University, Moscow, Russia, (2002).

[13] Entov, V.M., Turetskaya, F.D., and Voskov, D.V.: "On Approximaion of Phase Equilibria of Multicomponent Hydrocarbon Mixtuers and Prediction of Oil Displacements by Gas Injection", Eighth European Conference on the Mathematics of Oil Recovery, Freiburg, Germany, 4-7 Sep., (2001).

[14] Voskov, D.V., and Tchelepi, H.: "Compositional Space Parameterization for Flow Simulation", SPE 106029, 2007 SPE Reservoir Simulation Symposium, Woodlands, TX, February 26-28.

[15] Voskov, D.V., and Tchelepi, H.: "Compositional Space Parameterization for Miscible Displacement Simulation", *Transport in Porous Media*, (2007), DOI: 10.1007/s11242-008-9212-1

[16] Voskov, D.V., and Tchelepi, H.: "Compositional Parameterization for Multiphase Flow in Porous Media", SPE 113492, 2008 SPE/DOE Symposium on Improved Oil Recovery, Tulsa, Oklahoma, April 20-23.

[17] Gosset, R., Heyen G., and Kalitventzeff, B.: "An Efficient Algorithm to Solve Cubic Equations of State", *Fluid Phase Equilibria*, (1986), **25**, 51-64.

[18] Wang, P., Yotov, I., Wheeler, M., Arbogast, T., Dawson, C., Parashar, M., and Sepehrnoori, K.: "A New Generation EOS Compositional Reservoir Simulator: Part 1- Formuation and Discretization", SPE 37979, 1997 SPE Reservoir Simulation Symposium, Dallas, TX, June 8-11.

[19] Rasmussen, C.P., Krejbjerg, K., Michelesen, M.L., Bjurstrom, K.E.: "Increasing Computational Speed of Flash Calculations with Applications for Compositional Transient Simulations", SPE 84181, SPE Reservoir Evaluation and Engineering, Feb. (2006).

[20] Pope, S.B.: "Computationally Efficient Implementation of Combustion Chemistry Using In situ Adaptive Tabulation", Combust, Theory Modelling 1, (1997), 41-63.

[21] Firoozabadi, A., and Pan, H.: "Fast and Robust Algorithm for Compositional Modeling: Part I: Stability Analysis Testing", SPE Journal Mar. (2002), **7**, 78-89.

[22] Cao, H.: *Development of Techniques for General Purpose Simulators*, PhD thesis, Stanford University, (2002).

[23] Gong, B., Karimi-Fard, M., and Durlofsky, L.J.: "An Upscaling Procedure for Constructing Generalized Dual-porosity/Dual-permeability Models from Discrete Fracture Characterizations", SPE 102491, 2007 SPE Annual Technical Conference and Exhibition, San Antonio, TX, Sep. 24-27.

[24] Kenyon, D., and Behie, G.A.: "Third SPE Comparative Solution Project: Gas Cycling of Retrograde Condensate Reservoirs", SPE 11278, proceedings of the seventh SPE Symposium on Reservoir Simulation, San Francisco, CA, Nov. 15-18, (1983).

[25] Killough, J.E., and Kossack, C.A.: "Fifth Comparative Solution Project: Evaluation of Miscible Flood Simulators", SPE 16000, The Ninth SPE Symposium on Reservoir Simulation, San Antonio, TX (1987).

Appendix A

User's Guide to CSAT in GPRS

A.1 Keywords

We first describe the keywords associated with the usage of the Compositional Space Adaptive Tabulation (CSAT) technique at Stanford's General-Purpose Research Simulator (GPRS).

Currently, CSAT can be activated for an iso/thermal compositional problem for which thermodynamic interactions take place between two phases. The following is an example of the usage of the `CSAT` keyword:

```
CSAT
#ISCSAT    NPRES      PRESMIN    PRESMAX    NTEMP      TEMPMIN    TEMPMAX
    1        15         100       1800       10         619        711
#EPSCHECK EPSBNDRY  CRITRATIO REFINEDDP
   1e-2     2e-2        10         100
```

When the `CSAT` keyword followed by 11 parameters is not present in the input file for the reservoir, standard compositional procedures will be followed by default. Below, we explain each of these parameters in their correct order:

- `ISCSAT:` Flag to use CSAT `(1, 2)` or not `(0)`. When it is set to `2`, tie-line information will be written to output files.

- `NPRES:` Number of inclusive pressure levels in the pressure interval of the simulation (always greater than `1`). It depends on the size of the pressure interval; however, a value in the range of `10-20` is typical (`15` in the example above).

- `PRESMIN:` Minimum pressure of the simulation; which is normally, close to the pressure at the producer. When *MCP* for a temperature level is too small (close to or smaller than `PRESMIN`), a smaller `PRESMIN` may be required.

- `PRESMAX:` Maximum pressure of the simulation; which is normally, close to the pressure at the injector. When *MCP* for a temperature level is close to `PRESMAX`, a larger value may be required. This can be recognized by problems in the computation of tie-line tables, which essentially reduce the effectiveness of the simulation.

- `NTEMP:` Number of inclusive temperature levels in the temperature interval of a thermal simulation. The value depends on the size of the temperature interval; however, a value in the range of `10-20` is typical. For complicated thermal problems, a large value of `NTEMP (e.g. 30-50)` is suggested. For isothermal simulation, `NTEMP` could be set to `1`.

- `TEMPMIN:` Minimum temperature in the simulation.

- `TEMPMAX:` Maximum temperature in the simulation. For isothermal simulation, `TEMPMIN` and `TEMPMAX` could equal the temperature of the displacement. These four parameters define the regular grid in (2.17). It is worth mentioning that the lower and upper limits on p and T should support a larger $p - T$ region than the values suggested by the boundary conditions of a thermal problem.

  Note: If during the simulation, a pressure or temperature value outside the user-defined interval is encountered, a warning message will suggest the modification of `PRESMIN`, `PRESMAX`, `TEMPMIN` or `TEMPMAX`.

- `EPSCHECK:` Tolerance to check the closeness of a composition point to the interpolated

tie-line. A value in the range of `(0.005-0.05)` is typical, and smaller values may largely increase the number of calculated tie-lines. The checking criterion is defined in (2.13).

- `EPSBNDRY:` In order to resolve possible convergence issues in the overall Newton iteration, additional negative flash is performed for compositions which are too close to the two-phase envelope. `EPSBNDRY` defines the closeness of a composition point to the two-phase boundary. Considering the fact that the shape of the two-phase boundary may considerably change between the composition point and its adjacent tie-line, `EPSBNDRY` should be larger than `EPSCHECK` by several times (See [16, figure 2]). A value in the range of `(0.01-0.1)` is suggested. When it is set to zero, no negative flash will be performed and CSAT results will be used in the simulation; however, this may cause convergence problems. CSAT results will precondition negative flash if a large value of `EPSBNDRY (e.g. 100)` is used

- `CRITRATIO:` Ratio of `flashSwitchEps` to modify the switch from SSI to Newton in flash calculation of near-critical compositions. A value larger than `1` is suggested to perform fewer SSI iterations.

- `REFINEDDP:` The support of the refined table below *MCP* for each temperature level (See figure 2.9 and equation 2.14). A value of `100` is typical.

It should be noted that tuning these parameters (specially checking tolerances) could be a difficult task and some care is required to avoid ineffective simulation.

A.2 Simulation Output

Some information regarding the tie-line based simulation is provided in the performance section. Below is a typical example:

```
---- CSP input parameters ----
NPRES          15   PRESMIN     500   PRESMAX    4010
NTEMP          15   TEMPMIN     529   TEMPMAX     651
EPSCHECK     0.01  EPSBNDRY    0.02 CRITRATIO      10 REFINEDDP     100

---- CSP timing report ----
generating new table    13.143 sec ( 46%)
critical table check     0.984 sec (  3%)
subcritical CSAT         0.752 sec (  2%)
negative flash          13.087 sec ( 46%)
total CSP time          27.966 sec (100%)

---- CSP counters ----
                                        calls to routine
super-critical state         469712  72%        3468677  13%
ID by refined check             928   0%          35250   2%
ID by mixed check               173   0%           3196   5%
sub-critical state           174095  26%        1317907  13%
new TL calc.                     25   0%             25 100%
calls to CSAT                644933 100%

calls to negative flash      82220, of which 100% converged
# SSI iterations            924464, # Newton iterations          88888
# tie-line tables              25, # MCP calculations              200

---- Total EoS counters ----
flash iters SSI    =     937667, flash iters Newton =      91567
Stab. iters SSI    =     762395, Stab. iters Newton =      26520
```

Input parameters for CSAT are first presented. Timing report of CSAT routines (calculating new tables, checking critical and subcritical tie-lines and additional negative flash) is then summarized. `CSP counters` shows the number of calls to the routines in the same order they are called in a CSAT simulation. Number of calls to state identification routines along with successful call percentages are presented in the last two columns of `CSP counters`. The first two columns display the number of composition points at different states (super-, near- or sub-critical) identified by various routines. The percentages in the second column provide an idea about the distribution of compositions in the simulation.

Afterwards, the number of calls to preconditioned negative flash, percentage of successful returns and the associated number of SSI and Newton iterations are summarized. This

information includes only the flash performed by CSAT. Total number of *MCP* computations is at most the number of tie-line tables multiplied by `NTEMP`. Finally, SSI and Newton counters for stability test and flash calculations (in the entire simulation) compare the overall performance of tie-line based simulation with respect to the standard simulation (which should be run separately).

Two files are written which save the compositions of tie-line tables calculated in the course of the simulation. `tie_lines.out` includes tie-line compositions of all regular tables. Tie-lines are categorized using table number, temperature and pressure indices. In order to visualize the table information, refer to figures (2.3) and (2.8). It should be noted that the number of pressure levels is `NPRES+1`. `tie_lines_crit.out` stores near-critical tie-line compositions at different pressure levels with logarithmic approach to the associated *MCP* (refined table). Tie-lines with zero composition in `tie_lines.out` indicate the associated pressure value is above the *MCP* and in `tie_lines_crit.out` indicate that the corresponding temperature level is completely below *MCP* (which is by default `0`).

Note: In order to run SPE5 with standard EoS methods, `sinPhCrit` in `mthCompFluidModel.cpp` should set to be `MIXTC`.